Performance improvement and limitations in extremum seeking control ☆

Miroslav Krstić *

Department of Mechanical and Aerospace Engineering, University of California, San Diego, La Jolla, CA 92093-0411, USA

Abstract

We propose the inclusion of a dynamic compensator in the extremum seeking algorithm which improves the stability and performance properties of the method. This compensator is added to the integrator used for adaptation to improve the overall relative degree and phase response of the extremum seeking loop. The compensator is potentially more effective in accounting for the plant dynamics than the often used phase shifting of the demodulation signal. We present a detailed analysis of the extremum seeking system based on averaging. This analysis provides two linear models, one for tracking reference changes and the other for sensitivity to noise, which offer insight into how different parameters influence the performance. This analysis is less conservative than in previous cases and allows the use of faster adaptation for improved transients. We extend the extremum seeking method to problems of tracking changes in the set point which are more general than step functions. © 2000 Published by Elsevier Science B.V. All rights reserved.

Keywords: Extremum seeking; Overaging

1. Introduction

Despite a large amount of research effort expended during the period between the 1940s and 1970s [2,4–6,8,11,12,14–16], and despite considerable success in practice [3,10,17], the methods of "extremum seeking" are still in need of a much firmer theoretical foundation. Two available surveys on extremum seeking control, the one by Sternby [17] and Section 13.3 in [1], point at a lack of stability guarantees and clear design guidelines.

Pioneering work on stability analysis based on averaging in an extremum seeking system dates back to Meerkov [13]. In [9] we presented the first stability analysis for a problem with a *general nonlinear dynamical plant* which involves the use of both averaging and singular perturbations. However, the conditions imposed were restrictive: the plant had to be very fast (quasi-static) — albeit a completely general nonaffine nonlinear system — and the adaptation gain had to be small. In this paper we present a tighter analysis which removes these conditions, and propose dynamic compensation for providing stability guarantees, fast tracking of changes in the operating point, and measurement noise rejection.

* Tel.: 858-822-1374; fax: 858-534-7078.
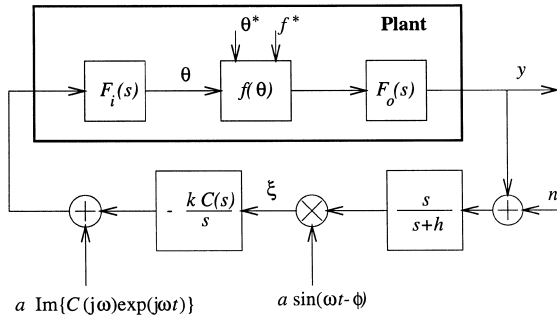*E-mail address:* krstic@ucsd.edu (M. Krstić)

Fig. 1. Implementation of the extremum seeking algorithm with compensation.

The paper opens in Section 2 with a motivation for incorporating dynamic compensation in the extremum seeking algorithm. Section 3 gives a summary of some basic properties of linear time-periodic systems that are used throughout the paper. Section 4 is the core of the paper where we derive average linearized models of the closed-loop system. In Section 5 we give an extension of the extremum seeking algorithm to tracking of changes in the unknown optimal operating point. In Section 6 we discuss how the theoretical results of the paper influence possible choices of design parameters in the extremum seeking algorithm, and in Section 7 we give a case study of the influence of the design parameters in the extremum seeking compensator.

2. Extremum seeking algorithm with dynamic compensation

We start with Fig. 1 which shows the implementation of the extremum seeking algorithm. The algorithm is applied to a plant that has an equilibrium map with an extremum. Without loss of generality, we assume that this extremum is a minimum, in which case we use $k > 0$. In case it is a maximum, the adaptation gain k would be negative. The plant is represented as a cascade combination of linear dynamics and a static nonlinearity. Within this limited class of systems, the linear dynamics are allowed to appear both at the input and at the output. Both of the linear blocks, $F_i(s)$ and $F_o(s)$, will be required to be stable. The output block $F_o(s)$ will be much more difficult to handle. It is crucial to note that all of the plant components are allowed to be *unknown*.

The only difference between the scheme in Fig. 1 and that in [9] is that the new scheme employs a compensator $C(s)$ in the adaptation law. This compensator will be used to improve the stability properties of the extremum seeking scheme and, in particular, remove the requirement that the adaptation gain k be small. The effect of this compensator will be similar to adding derivative action to a proportional controller to improve the damping. Similarly, this compensator can be regarded as a phase-lead compensator which improves the phase margin in a loop with a high relative degree. One limitation to the speed of adaptation will be imposed by the presence of the measurement noise input n.

The periodic perturbations used in the loop perform modulation and demodulation, and their role is to make the extremum of the equilibrium map, which is flat and therefore appears as a zero gain block, appear, in a time-average sense, as a gain proportional to the second derivative at the extremum. The role of the washout filter $s/(s + h)$ is to eliminate the bias to the DC component of the equilibrium map.

The static nonlinear block $f(\theta)$ is assumed to have a minimum for $\theta = \theta^*$. From the Taylor expansion

$$f(\theta) = f(\theta^*) + f'(\theta^*)(\theta - \theta^*) + \tfrac{1}{2}f''(\theta^*)(\theta - \theta^*)^2 + \mathrm{O}((\theta - \theta^*)^3) \tag{1}$$

with the minimum assumption $f'(\theta^*) = 0$, and by dropping the terms of order three and higher, we get

$$f(\theta) = f(\theta^*) + \tfrac{1}{2}f''(\theta^*)(\theta - \theta^*)^2. \tag{2}$$

By appropriate renormalization of the problem, one can absorb $f''(\theta^*)/2$ into the integrator gain k. Denoting $f(\theta^*) = f^*$, we get

$$f(\theta) = f^* + (\theta - \theta^*)^2. \tag{3}$$

In this format, f^* and θ^* can be regarded as disturbance inputs.

Before we proceed to our detailed analysis, this is a good place to make a comment about the style of analysis and notation. Strictly speaking, we cannot say that expressions (1) and (2) are equal because they differ by $O((\theta - \theta^*)^3)$. However, to keep the presentation simple, in the sequel, the equality sign will mean both equal and "approximately equal". The approximateness may be in terms of neglected higher-order terms, or in terms of averaging approximations (which are valid for high ω). All of the statements that we will be making can be interpreted in terms of rigorous averaging and local stability theorems. The reason we do not pursue these interpretations here as in [9] is ease of presentation.

Another convention we will follow for ease of presentation is a combined use of time- and frequency-domain symbols. In particular, a transfer function in front of a bracketed time function, such as $G(s)[u(t)]$, means a time-domain signal obtained as an output of $G(s)$ driven by $u(t)$.

3. Lemmas on modulation

In the sequel, we will need the following two lemmas. The symbol ε^{-t} represents exponentially decaying terms.

Lemma 3.1. *If the transfer function $H(s)$ has all of its poles with negative real parts, then, for any real ψ,*

$$H(s)[\sin(\omega t - \psi)] = \text{Im}\{H(j\omega)e^{j(\omega t - \psi)}\} + \varepsilon^{-t}. \tag{4}$$

Proof. This is a standard modulation property of the Laplace transform. We give its proof because of its importance and for convenience of the reader:

$$H(s)[\sin(\omega t - \psi)] = H(s)[\text{Im}\{e^{j(\omega t - \psi)}\}]$$

$$= \frac{1}{2j}H(s)[e^{j(\omega t - \psi)} - e^{-j(\omega t - \psi)}]$$

$$= \frac{1}{2j}\mathcal{L}^{-1}\left\{H(s)\frac{1}{s - j\omega}e^{-j\psi} - H(s)\frac{1}{s + j\omega}e^{j\psi}\right\}$$

$$= \frac{1}{2j}\mathcal{L}^{-1}\left\{H(j\omega)\frac{1}{s - j\omega}e^{-j\psi} - H(-j\omega)\frac{1}{s + j\omega}e^{j\psi}\right.$$

$$\left. + \text{partial fractions due to } H(s)\right\}$$

$$= \frac{1}{2j}(H(j\omega)e^{j(\omega t - \psi)} - H(-j\omega)e^{-j(\omega t - \psi)}) + \varepsilon^{-t}$$

$$= \text{Im}\{H(j\omega)e^{j(\omega t - \psi)}\} + \varepsilon^{-t}. \quad \square \tag{5}$$

Lemma 3.2. *If the transfer functions $G(s)$ and $H(s)$ have all of their poles with negative real parts, the following statement is true for any real ϕ and any uniformly bounded $z(t)$:*

$$G(s)[(H(s)[\sin(\omega t - \phi)])z(t)] = \text{Im}\{e^{j(\omega t - \phi)}H(j\omega)G(s + j\omega)[z(t)]\} + \varepsilon^{-t}. \tag{6}$$

Proof. The lemma is proved using the following straightforward calculation:

$$G(s)[(H(s)[\sin(\omega t - \phi)])z(t)] = G(s)[\text{Im}\{H(j\omega)e^{j(\omega t - \phi)}\}[z(t)] + \varepsilon^{-t}] \quad \text{(by Lemma 1)}$$

$$= \text{Im}\{e^{-j\phi}\mathscr{L}^{-1}\{G(s)H(j\omega)Z(s - j\omega)\}\} + \varepsilon^{-t}$$

$$= \text{Im}\{e^{j(\omega t - \phi)}H(j\omega)\mathscr{L}^{-1}\{G(s + j\omega)Z(s)\}\} + \varepsilon^{-t}$$

$$\text{(by definition of Laplace transform)}$$

$$= \text{Im}\{e^{j(\omega t - \phi)}H(j\omega)G(s + j\omega)[z(t)]\} + \varepsilon^{-t}. \qquad \square \tag{7}$$

The following easily verifiable statement is formulated as a lemma for convenient reference.

Lemma 3.3. *For any rational functions* $A(\cdot)$ *and* $B(\cdot, \cdot)$ *the following is true*:

$$\text{Im}\{e^{j(\omega t - \psi)}A(j\omega)\}\text{Im}\{e^{j(\omega t - \phi)}B(s, j\omega)[z(t)]\}$$

$$= \tfrac{1}{2}\text{Re}\{e^{j(\psi - \phi)}A(-j\omega)B(s, j\omega)[z(t)]\} - \tfrac{1}{2}\text{Re}\{e^{j(2\omega t - \psi - \phi)}A(j\omega)B(s, j\omega)[z(t)]\}. \tag{8}$$

4. Average linear models

In this section we develop tools for studying stability of the improved extremum seeking scheme. Of course, one can test the scheme for stability by running a simulation of the complete nonlinear time-varying system. The analysis we develop here reduces the problem to testing stability of a linearized average (LTI) model, which can be done as a simple algebraic test, rather than a simulation. Such models are rigorously developed in this section, and it is indicated under what conditions their stability implies (based on the averaging theorem) convergence towards a vicinity of the extremum point.

Suppose $C(s)$, $F_i(s)$, and $F_o(s)$ are all asymptotically stable. We start with the equations governing the model in Fig. 1:

$$y = F_o(s)[f^* + (\theta - \theta^*)^2], \tag{9}$$

$$\theta = F_i(s)C(s)\left[a\sin\omega t - \frac{k}{s}[\xi]\right], \tag{10}$$

$$\xi = a\sin(\omega t - \phi)\frac{s}{s + h}[y + n], \tag{11}$$

where (10) follows from applying Lemma 3.1 with $H(s) = C(s)$ and $\psi = 0$. Let us denote

$$\theta_0(t) = F_i(s)C(s)[a\sin\omega t], \tag{12}$$

$$\tilde{\theta} = \theta^* - \theta + \theta_0(t), \tag{13}$$

$$\tilde{y} = y - F_0(s)[f^*]. \tag{14}$$

First we derive an average model for $\tilde{\theta}$ and then for $\tilde{y}$.

Lengthy calculations based on the above equations and employing Lemmas 3.1–3.3 lead to the following relationship:

$$\tilde{\theta} + ka^2 F_i(s)C(s)\frac{1}{s}\left[\text{Re}\left\{e^{j\phi}F_i(j\omega)C(j\omega)\frac{s + j\omega}{s + j\omega + h}F_o(s + j\omega)[\tilde{\theta}]\right\}\right]$$

$$= \theta^* + \varepsilon, \tag{15}$$

where

$$\varepsilon = kaF_i(s)C(s)\frac{1}{s}\left[\sin(\omega t - \phi)\frac{s}{s+h}[F_o(s)[f^*] + n + a^2(F_i(s)C(s)[\sin\omega t])^2 + \tilde{\theta}^2]\right]$$
$$- ka^2F_i(s)C(s)\frac{1}{s}\left[\operatorname{Re}\left\{e^{j(2\omega t - \phi)}F_i(j\omega)C(j\omega)\frac{s+j\omega}{s+j\omega+h}F_o(s+j\omega)[\tilde{\theta}]\right\}\right]. \tag{16}$$

In this calculation we have neglected the exponentially decaying terms.[1] We have reduced the system to a form where the left-hand side of (15) is LTI, and only ε is time varying and nonlinear. Next, we determine the average model. For averaging to be applicable ω must be large relative to all other parameters in the problem. For constant f^*, n the average of (16) is

$$\operatorname{Ave}\{\varepsilon\} = \operatorname{Ave}\left\{kaF_i(s)C(s)\frac{1}{s}\left[\sin(\omega t - \phi)\frac{s}{s+h}[a^2(F_i(s)C(s)[\sin\omega t])^2]\right]\right\}$$
$$= O(ka^3). \tag{17}$$

The operator $\operatorname{Ave}\{\cdot\}$ is defined as follows:

1. represent system (16) in the state space form;
2. average the right-hand side of the state equation with respect to time over the period $2\pi/\omega$ treating the states and the 'input' $\tilde{\theta}$ as constants;
3. compute the output, as a function of time, of the average (autonomous) system.

Thus we arrive at the following proposition.

Proposition 4.1. *For the system in Fig.* 1, *the average linearized model relating* θ^* *and* $\tilde{\theta}$ *is*

$$\frac{\tilde{\theta}(s)}{\theta^*(s)} = \frac{1}{1+L(s)}, \tag{18}$$

where

$$L(s) = ka^2/2\left(e^{j\phi}\frac{s+j\omega}{s+j\omega+h}F_o(s+j\omega)F_i(j\omega)C(j\omega)\right.$$
$$\left. + e^{-j\phi}\frac{s-j\omega}{s-j\omega+h}F_o(s-j\omega)F_i(-j\omega)C(-j\omega)\right)F_i(s)C(s)\frac{1}{s}. \tag{19}$$

The average model (18) can be used to test for stability of the extremum seeking system. The conclusions of this test can be stated in the form of a theorem based on the averaging theorem [7, Theorem 8.3], as we had done in [9]. We do not give such a formal theorem here because it would require the introduction of a great deal of extra state space notation. For completeness, we just indicate here the qualitative statement. If the average model is asymptotically stable, $1/\omega$ is sufficiently small and the initial conditions are small in an appropriate sense, then the theorem would claim the existence of an exponentially stable periodic solution which is at a distance that continuously depends on $1/\omega$, a, and k.

Following the configuration in Fig. 1, one would now be tempted, based on intuition for LTI feedback systems, to expect that the average transfer function from the disturbance $n+F_o(s)[f^*]$ to the output error $\tilde{y}$ be

$$\frac{\tilde{y}(s)}{n(s)+F_o(s)f^*(s)} = -\frac{L(s)}{1+L(s)}. \tag{20}$$

This is however not the case at all. The nonlinear time-varying nature of the system prevents us from using one average system to obtain another. The correct result happens to be, however, as stated in the following proposition.

---

[1] Note that these terms are not only additive but also multiplicative. The multiplicative terms cannot destroy stability. This can be seen using a standard Gronwall lemma type argument.
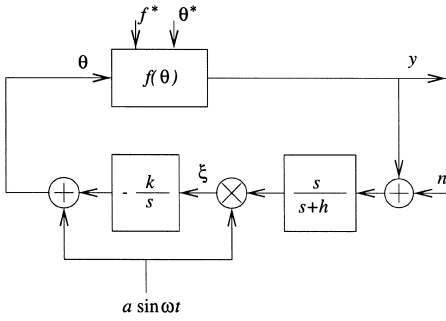
Fig. 2. Example.

Proposition 4.2. *For the system in Fig.* 1, *the average linearized model relating* $F_o(s)[f^*] + n$ *and* $\tilde{y}$ *is*

$$\frac{\tilde{y}(s)}{n(s) + F_o(s)f^*(s)} = -\frac{M(s)}{1 + M(s)}, \tag{21}$$

where

$$M(s) = ka^2/2\frac{s}{s+h}F_o(s)\left(e^{-j\phi}F_i(-j\omega)C(-j\omega)\frac{F_i(s+j\omega)C(s+j\omega)}{s+j\omega}\right. $$
$$\left. + e^{j\phi}F_i(j\omega)C(j\omega)\frac{F_i(s-j\omega)C(s-j\omega)}{s-j\omega}\right). \tag{22}$$

This is obtained by first deriving the relationship

$$\tilde{y} = -ka^2 F_o(s)\left[(F_i(s)C(s)[\sin\omega t])\frac{F_i(s)C(s)}{s}\left[\sin(\omega t - \phi)\left(\frac{s}{s+h}[\tilde{y} + F_o(s)[f^*] + n]\right)\right]\right]$$
$$+ \delta, \tag{23}$$

where

$$\delta = F_o(s)[-2\theta_0\theta^* + \tilde{\theta}^2 + \theta_0^2]. \tag{24}$$

Noting that δ has an $O(\tilde{\theta}^2 + a^2)$ average, and using Lemmas 3.1– 3.3, we obtain the linearized average system in the form (21).

The difference between the loop transfer functions $L(s)$ and $M(s)$ (which in an LTI analysis would be expected to be the same) is striking. This difference gives rise to different stability criteria for the average system (21) and (18).

As surprising as it may be, the difference between the two average systems is not difficult to explain. The two representations of the same system in Fig. 1, for which we derived average models, are related by a *time-varying* change of coordinates (in fact, there are two different changes of coordinates depending on whether we are expressing $\tilde{y}$ in terms of $\tilde{\theta}$ or vice versa). Thus, one cannot expect the average systems to be equivalent.

Example 4.1. Let us consider a system with $C(s) = F_i(s) = F_o(s) = 1$ and $\phi = 0$ given in Fig. 2. This system is the simplest example of an extremum seeking problem where the plant is just a static map and the seeking algorithm does not employ any compensation or demodulator phase shift. The $\tilde{\theta}$ average model is

$$\frac{\tilde{\theta}(s)}{\theta^*(s)} = \frac{s(s^2 + 2hs + h^2 + \omega^2)}{s^3 + (2h + ka^2)s^2 + (h^2 + \omega^2 + ka^2h)s + ka^2\omega^2} \tag{25}$$

and the $\tilde{y}$ average model is

$$\frac{\tilde{y}(s)}{n(s) + f^*(s)} = -ka^2\frac{s^2}{s^3 + (h + ka^2)s^2 + \omega^2 s + \omega^2 h}. \tag{26}$$
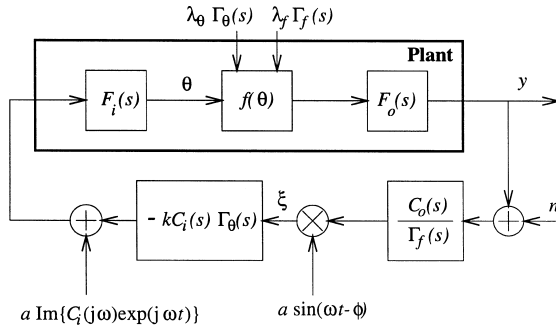
Fig. 3. Extension of the extremum seeking algorithm to non-step changes in θ^* and f^*.

A Routh test shows that both transfer functions are asymptotically stable for all $k > 0$ (although, it should be noted that the averaging approximation is valid only when ka^2 is small relative to ω). However, a simple root locus analysis shows different behavior between the two transfer functions. For small h the $\tilde{\theta}$ system will have a dipole near the imaginary axis, which means that a pair of closed-loop poles will be lightly damped but their influence on the time response will be minor. On the other hand, the $\tilde{y}$ system will have two lightly damped closed-loop poles which are not due to a dipole. This happens for large ω, which means that for large ω the system will be sensitive to measurement noise. A large value of ka^2 will dampen these poles but it will introduce two closed-loop poles near the origin (and, as mentioned above, for large ka^2 the averaging ceases to be valid). This example shows that possible benefits of increasing the adaptation gain to tracking changes in θ^* are accompanied by increased sensitivity to noise.

5. Generalized scheme for problems with nonstep changes in θ^* and f^*

Suppose a change in the plant operating condition (characterized by either θ^* or f^*) is not an abrupt step change but a more gradual ramp change. In that case, we would appropriately include this information in the extremum seeking compensator. Let

$$\mathscr{L}\{\theta^*(t)\} = \lambda_\theta \Gamma_\theta(s), \tag{27}$$

$$\mathscr{L}\{f^*(t)\} = \lambda_f \Gamma_f(s). \tag{28}$$

where $\Gamma_\theta(s), \Gamma_f(s)$ are known functions, and $\lambda_\theta, \lambda_f$ are *unknown* constants. The generalized extremum seeking scheme is shown in Fig. 3. For implementation, the compensators $C_i(s)$ and $C_o(s)$ should be chosen so that $C_i(s)\Gamma_\theta(s)$ and $C_o(s)/\Gamma_f(s)$ are *proper transfer functions*. With this generalized scheme we have

$$L(s) = ka^2/2 \left(e^{j\phi} \frac{C_o(s+j\omega)}{\Gamma_f(s+j\omega)} F_o(s+j\omega) F_i(j\omega) C_i(j\omega) \right.$$

$$\left. + e^{-j\phi} \frac{C_o(s-j\omega)}{\Gamma_f(s-j\omega)} F_o(s-j\omega) F_i(-j\omega) C_i(-j\omega) \right) F_i(s) C_i(s) \Gamma_\theta(s) \tag{29}$$

and

$$M(s) = ka^2/2 \frac{C_o(s)}{\Gamma_f(s)} F_o(s) (e^{-j\phi} F_i(-j\omega) C_i(-j\omega) F_i(s+j\omega) C_i(s+j\omega) \Gamma_\theta(s+j\omega)$$

$$+ e^{j\phi} F_i(j\omega) C_i(j\omega) F_i(s-j\omega) C_i(s-j\omega) \Gamma_\theta(s-j\omega)). \tag{30}$$
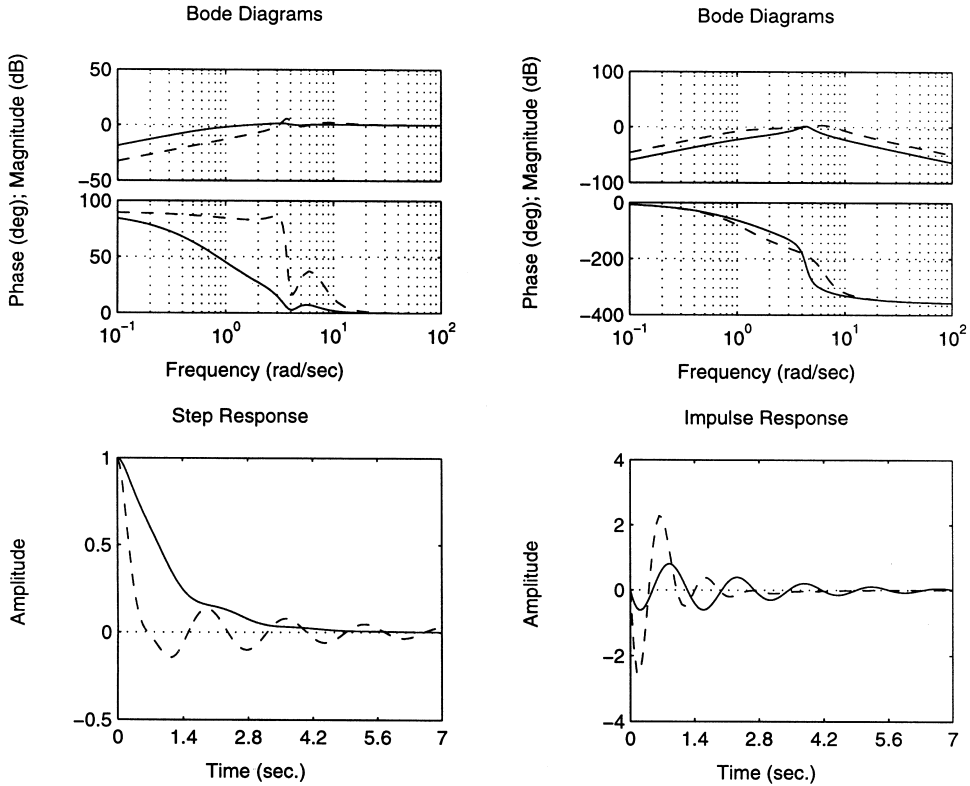
Fig. 4. Results for $\tau = 0$ and $q = 3$ (solid) and $q = 15$ (dashed). The plots on the left correspond to the transfer function $1/(1 + L(s))$ and the plots on the right are for the transfer function $-M(s)/(1 + M(s))$.

The inclusion of transfer functions $\Gamma_\theta(s)$ and $\Gamma_f(s)$ into the extremum seeking loop achieves the cancellation of the poles of $\Gamma_\theta(s)$ and $\Gamma_f(s)$, viz.,

$$\tilde{\theta}(s) = \frac{1}{1 + L(s)} \mathscr{L}\{\theta^*(t)\} = \lambda_\theta \frac{L^{-1}(s)}{1 + L^{-1}(s)} \Gamma_\theta(s), \tag{31}$$

$$\tilde{y}(s) = -\frac{M(s)}{1 + M(s)} \mathscr{L}\{f^*(t)\} = -\lambda_f \frac{M(s)}{1 + M(s)} \Gamma_o(s)\Gamma_f(s), \tag{32}$$

so that $\tilde{\theta}(t)$ and $\tilde{y}(t)$ exponentially decay to zero whenever the compensators $C_i(s)$ and $C_o(s)$ are selected so that all the zeros of the transfer functions $1 + L(s)$ and $1 + M(s)$ have negative real parts. Note that some tracking objectives, such as, for example, a ramp in $\theta^*(t)$, may make the stabilization problem quite difficult (by introducing a double integrator in $\Gamma_\theta(s)$).

6. Design considerations

Let us now return to the basic extremum seeking scheme given in Fig. 1 and analyzed in Section 4. The essence of the results in Proposition 4.1 is that, the closed-loop system will be asymptotically stable if all the zeros of the transfer function $1 + L(s)$ have negative real parts. This will be the case if and only if a negative
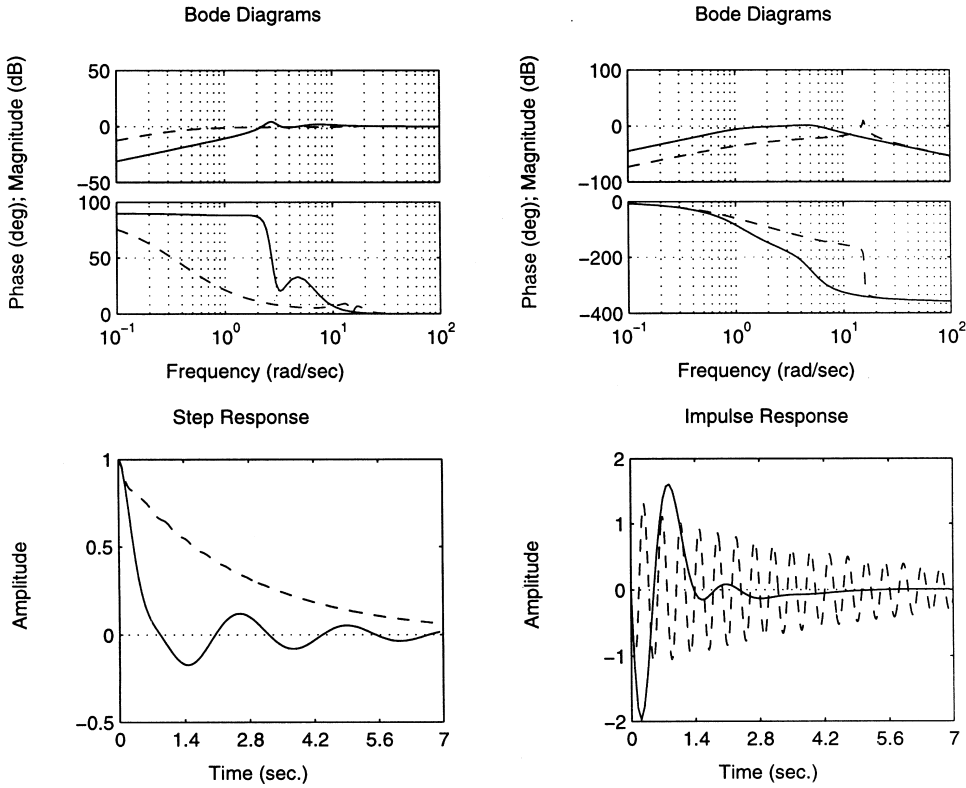
Fig. 5. Results for $\tau = 0$ and $\omega = 3$ (solid) and $\omega = 15$ (dashed). The plots on the left correspond to the transfer function $1/(1 + L(s))$ and the plots on the right are for the transfer function $-M(s)/(1 + M(s))$.

feedback system with the blocks

$$\frac{ka^2/2}{s} \tag{33}$$

and

$$\left(e^{j\phi} \frac{s + j\omega}{s + j\omega + h} F_o(s + j\omega) F_i(j\omega) C(j\omega) + e^{-j\phi} \frac{s - j\omega}{s - j\omega + h} F_o(s - j\omega) F_i(-j\omega) C(-j\omega) \right) F_i(s) C(s) \tag{34}$$

is asymptotically stable. Since the transfer function (33) – an integrator with a positive gain – is positive real, by the passivity theorem (see, for example, [7]), the feedback loop will be stable for all $k > 0$ provided the block (34) is strictly positive real. While it is intuitively clear how $C(s)$, ϕ, and h can be used to make (34) strictly positive real, it is hard to make this selection systematic.

Let us recall the necessary conditions for SPRness: the transfer function must be stable, minimum phase, and have relative degree no larger than one. Since the adaptation law $kC(s)/s$ must be proper (we cannot use pure differentiation), the relative degree of $C(s)$ must be at least -1. Then, for (34) to have relative degree no higher than one, it means that the relative degree of $F_o(s)F_i(s)$ can be at most two. Clearly, a compensator $C(s)$ of relative degree -1 will be typically of the proportional-derivative (PD) type.

The above discussion outlines a typical use of the compensator $C(s)$ – in situations where the overall relative degree of the plant and the integrator would exceed two, in which case high adaptation gain would drive two of the open loop poles into the right half-plane. The introduction of $C(s)$ would reduce the overall relative degree to two and allow the use of higher adaptation gain k for improving the convergence. Below, we discuss the disadvantages of excessively increasing k, and the underlying trade-offs.
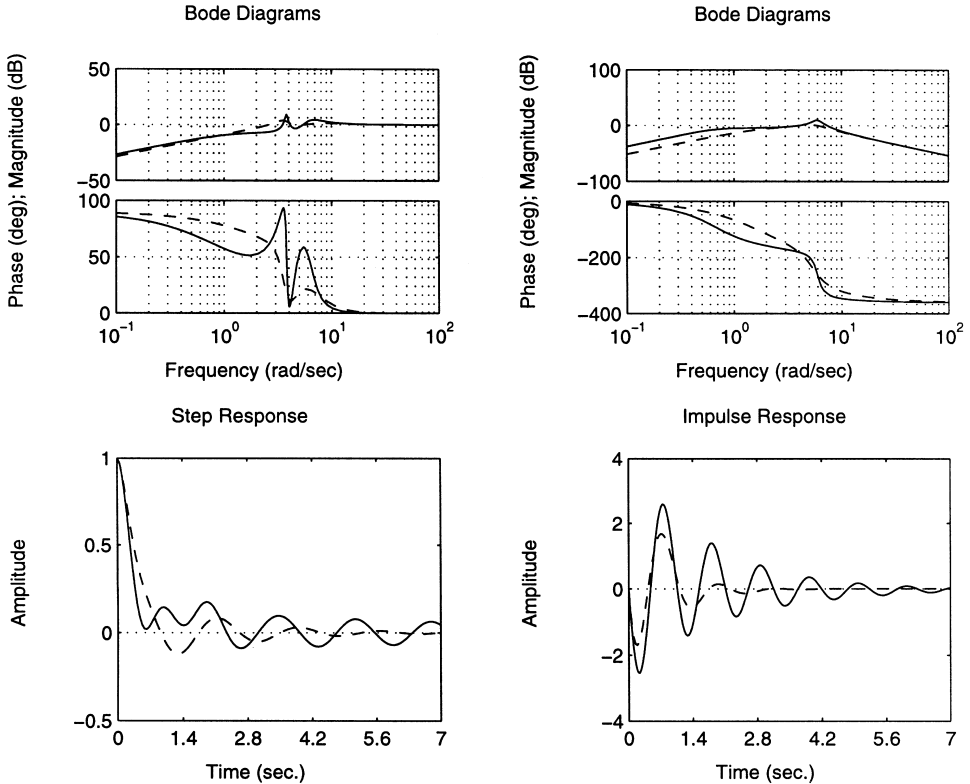
Fig. 6. Results for $\tau = 0$ and $h = 1$ (solid) and $h = 5$ (dashed). The plots on the left correspond to the transfer function $1/(1 + L(s))$ and the plots on the right are for the transfer function $-M(s)/(1 + M(s))$.

The compensator is equally useful when the plant is of relative degree one. In that case the loop gain without $C(s)$ is two and, under high k, the extremum seeking loop becomes lightly damped at best (or even unstable). This effect has been observed in numerous simulations and experiments by researchers working in this area who have registered overshoots and instabilities. The inclusion of a PD action through $C(s)$ improves the adaptation transients and stability properties.

However, there are situations where PD action via $C(s)$ is unnecessary and may even be harmful. For example, when the plant already has high bandwidth (for example, a lag-type plant with a fast pole), adding PD action will increase the bandwidth and make the system unnecessarily sensitive to noise. Similar effect with respect to noise can be expected in more difficult plants (those with higher relative degree). Adding a PD action via $C(s)$ would reduce overshoots and improve stability for reasonable values of the adaptation gain, but for excessive values it would make the adaptation contaminated by noise.

All the discussion thus far addresses only the interplay between the compensator, the plant, and the adaptation gain. There is however also a delicate balance between the sizes of the design parameters ka^2, and ω. In order for the averaging method to be applicable, ω should be large (in relative terms) with respect to ka^2. Also, the presence of the $O(ka^3)$ error in the $\tilde{\theta}$-system indicates that we should keep ka^2 moderate. On the other hand, small ka^2 will slow down the convergence.

It is also important to see that ω – and not only ka^2 – affects the speed of adaptation, because the speed of adaptation is proportional to $|F_i(j\omega)C(j\omega)|$. Typically, $F_i(s)C(s)$ will have some roll-off at high frequencies. Therefore, if ω is selected too high to satisfy the conditions of the averaging method, the convergence will be slow. Thus, a preferable value of ω is that which is just sufficient to separate the time scales of the perturbation signal $a \sin \omega t$ and the plant with the extremum seeking dynamics.
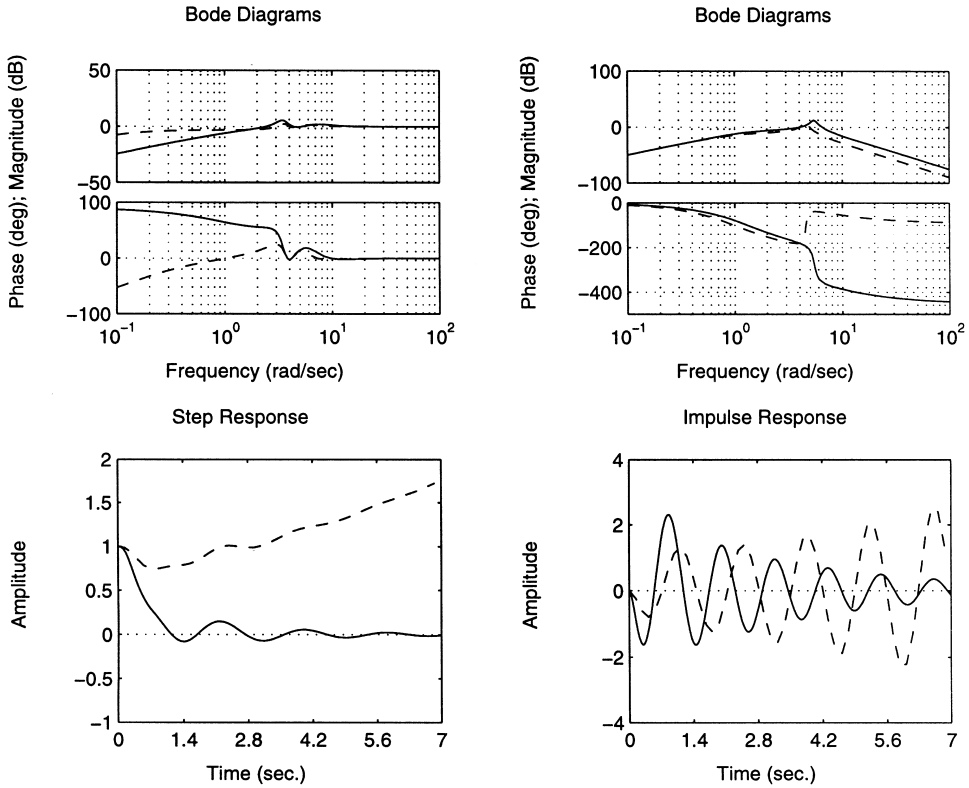
Fig. 7. Results for $\tau = 0.12$ (solid) and $\tau = 0.6$ (dashed). The plots on the left correspond to the transfer function $1/(1 + L(s))$ and the plots on the right are for the transfer function $-M(s)/(1 + M(s))$.

7. Example

In this section we consider the problem of extremum seeking for a plant with the transfer functions

$$F_i(s) = 1, \qquad F_o(s) = \frac{1}{(s + p)(\tau s + 1)}. \tag{35}$$

Throughout this section, p will have a fixed value $p = 1$ and τ will vary between zero and positive values. Unless specifically mentioned, the other quantities will have nominal values $q = ka^2/2 = 10$, $\omega = 4$, $h = 4$, $\phi = 0$, and $C(s) = 1$.

7.1. Influence of parameters ka^2, ω, and h

First, we consider the case where $\tau = 0$, in which case we use no compensation ($C(s) = 1$) and no phase shifting ($\phi = 0$), and illustrate only the effects of changing q, ω, and h. Fig. 4 show results for $q = 3$ and 15. The two Bode plots are for the transfer functions $1/(1 + L(s))$ (left) and $-M(s)/(1 + M(s))$ (right). These two transfer functions correspond, respectively, to the input–output relationships between θ^* and $\tilde{\theta}$, and n and $\tilde{y}$. Underneath the Bode plots we show, respectively, the step response of $\tilde{\theta}$ to the step input in the optimal parameter θ^*, and the impulse response of $\tilde{y}$ to the noise n (in terms of frequency content, a δ-impulse is representative of white measurement noise). We see in Fig. 4 that the increase of q improves the tracking of changes in θ^* but it also increases the sensitivity to noise.

Fig. 5 shows the effect of increasing ω for frequencies $\omega = 3$ (solid) and $\omega = 15$ (dashed). On the left we show the effects of changes in θ^* on the tracking error, and on the right the effect of measurement noise on
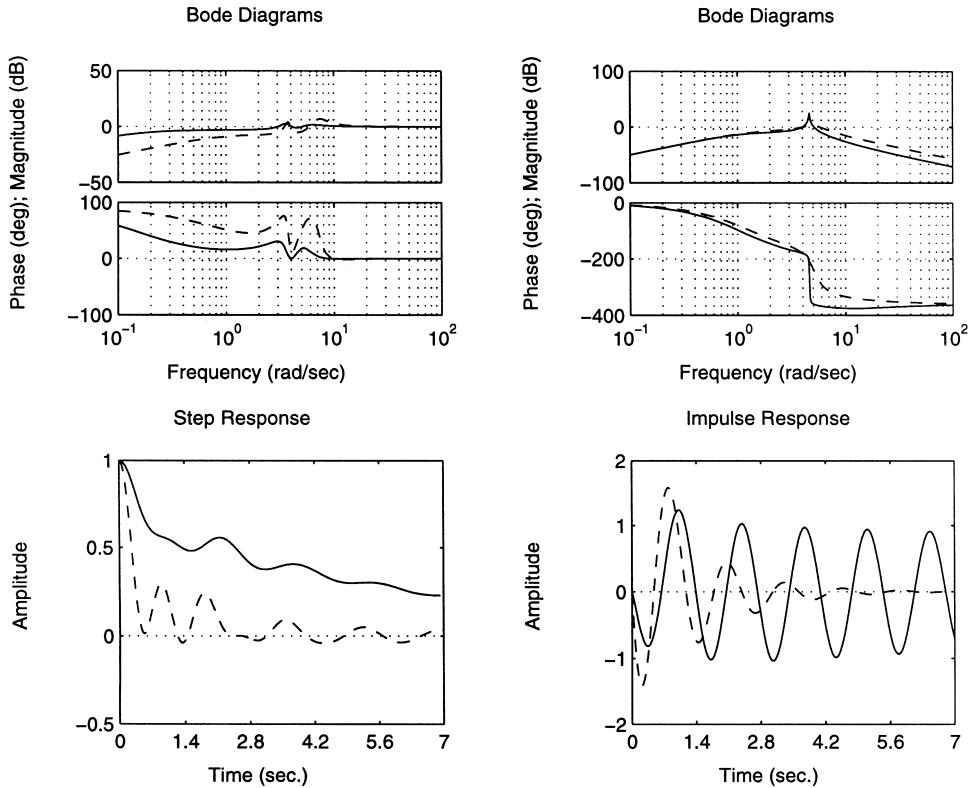
Fig. 8. Results for $\tau = 0.6$ and $d = 0.08$ (solid) and $d = 0.4$ (dashed). The plots on the left correspond to the transfer function $1/(1 + L(s))$ and the plots on the right are for the transfer function $-M(s)/(1 + M(s))$.

the output. The figure shows a trend that higher ω smoothes out the tracking response but makes the response to noise more oscillatory.

Fig. 6 shows the effect of increasing the cut-off frequency h of the high-pass filter $s/(s + h)$ for $h = 1$ (solid) and $h = 5$ (dashed). Even though h cannot be increased indiscriminately (in which case the filter would approach a pure differentiator), the figure shows that higher h improves the response.

From the above considerations we pick $q = 10$ and $\omega = h = 4$ as good values for the plant with $p = 1$ and $\tau = 0$, and with no compensator, $C(s) = 1$. Note that $C(s)$ is not needed because for $\tau = 0$, the overall extremum seeking loop is relative degree two.

7.2. Compensation for the relative degree two plant

Now we increase τ from zero to a positive value. Fig. 7 shows results for two different values of τ. The solid curves are for $\tau = 0.12$, a case where the closed-loop system is asymptotically stable. The dashed curves are for the value $\tau = 0.6$ for which the closed-loop system goes unstable. Besides the fact that the closed loop goes unstable for a larger number of τ (with $q = 10$, $\omega = h = 4$, and $C(s) = 1$), one should note that, from the root locus one can see that the closed loop is unstable even for arbitrarily small numbers of q (due to a positive zero and a pole near the origin in $L(s)$ and a pair of imaginary poles in $M(s)$).

Fig. 8 shows results for $\tau = 0.6$ in the presence of a dynamic compensator $C(s) = 1 + ds$ with $d = 0.08$ (solid) and $d = 0.4$ (dashed). We observe that the compensator stabilizes the plant and, for $d = 0.4$, achieves reasonably good tracking and noise rejection performance. For larger values of d, not shown here, the performance starts to deteriorate. It should be noted that the compensator is of the PD form, such that the overall adaptation
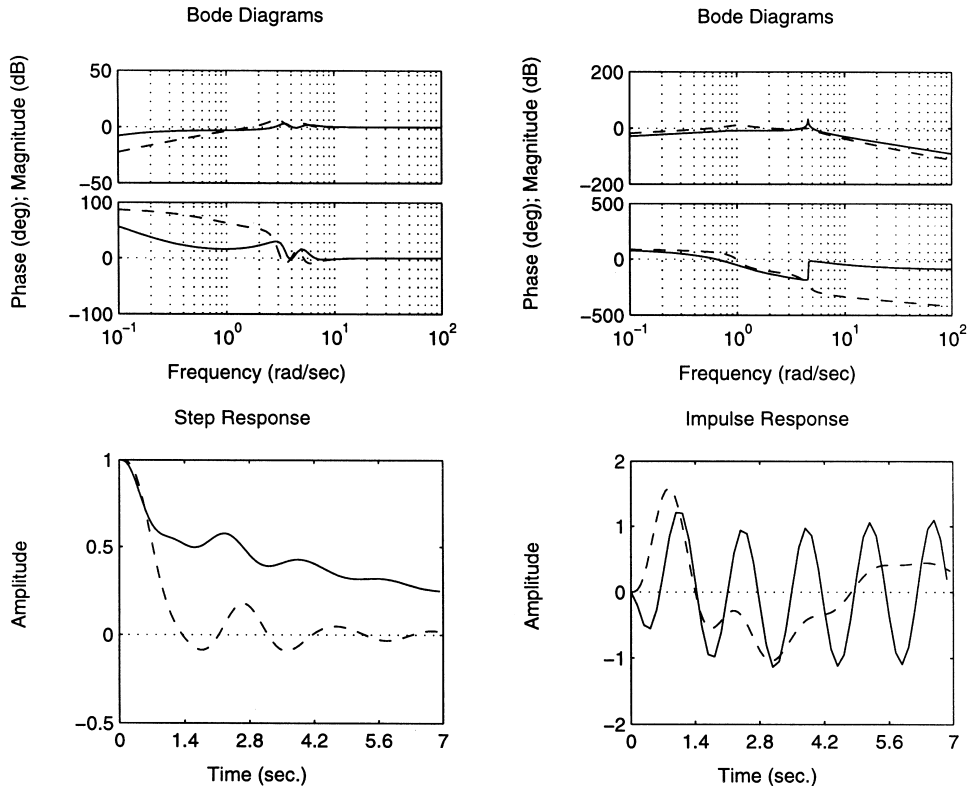
Fig. 9. Results for $\tau = 0.6$ and $\phi = 0.3$ (solid) and $\phi = 1.5$ (dashed). The plots on the left correspond to the transfer function $1/(1 + L(s))$ and the plots on the right are for the transfer function $-M(s)/(1 + M(s))$.

law $C(s)/s$ is a PI compensator. The derivative action in $C(s)$ provides a phase-lead effect necessary for stabilization and performance improvement.

Fig. 9 shows results for $\tau = 0.6$ in the absence of a dynamic compensator ($C(s) = 1$) with $\phi = 0.3$ (solid) and $\phi = 1.5$ (dashed). The dashed plots in this figure are not very different from the dashed plots in Fig. 8 and they show that the phase shift ϕ in the demodulation signal can, to some extent, help the stabilization and performance improvement tasks. However, this method of compensation for the plant dynamics is ridden with some other difficulties, an example of which is the appearance of a slow near-resonance in the noise-to-output transfer function, which gives the slow settling in the impulse response (dashed in Fig. 9).

References

[1] K.J. Astrom, B. Wittenmark, Adaptive Control, 2nd ed., Addison-Wesley, Reading, MA, 1995.

[2] P.F. Blackman, Extremum-seeking regulators, in: J.H. Westcott (Ed.), An Exposition of Adaptive Control, Macmillan, New York, 1962.

[3] C.S. Drapper, Y.T. Li, Principles of optimalizing control systems and an application to the internal combustion engine, ASME, vol. 160, pp. 1–16, 1951, also in: R. Oldenburger (Ed.), Optimal and Self-Optimizing Control, MIT Press, Boston, MA, 1966.

[4] A.L. Frey, W.B. Deem, R.J. Altpeter, Stability and optimal gain in extremum-seeking adaptive control of a gas furnace, Proceedings of the Third IFAC World Congress, vol. 48A, London, 1966.

[5] O.L.R. Jacobs, G.C. Shering, Design of a single-input sinusoidal-perturbation extremum-control system, Proc. IEE 115 (1968) 212–217.

[6] V.V. Kazakevich, Extremum control of objects with inertia and of unstable objects, Soviet Phys. Dokl. 5 (1960) 658–661.

[7] H.K. Khalil, Nonlinear Systems, 2nd ed., Prentice-Hall, Englewood Cliffs, NJ, 1996.

[8] A.A. Krasovskii, The Dynamics of Continuous Selfadaptive Systems, Gos. Izdat. Fiz.-Mat. Lit., Moscow, 1963 (in Russian).

[9] M. Krstić, H.H. Wang, Stability of extremum seeking feedback for general nonlinear dynamic systems, Automatica (2000), to appear.

[10] M. Leblanc, Sur l'electrification des chemins de fer au moyen de courants alternatifs de frequence elevee, Revue Generale de l'Electricite (1922).

[11] S.M. Meerkov, Asymptotic methods for investigating quasistationary states in continuous systems of automatic optimization, Automation Remote Control (11) (1967) 1726–1743.

[12] S.M. Meerkov, Asymptotic methods for investigating a class of forced states in extremal systems, Automation Remote Control (12) (1967) 1916–1920.

[13] S.M. Meerkov, Asymptotic methods for investigating stability of continuous systems of automatic optimization subjected to disturbance action, Avtomatika i Telemekhanika (12) (1968) 14–24 (in Russian).

[14] I.S. Morosanov, Method of extremum control, Automation Remote Control 18 (1957) 1077–1092.

[15] I.I. Ostrovskii, Extremum regulation, Automation Remote Control 18 (1957) 900–907.

[16] A.A. Pervozvanskii, Continuous extremum control system in the presence of random noise, Automation Remote Control 21 (1960) 673–677.

[17] J. Sternby, Extremum control systems: An area for adaptive control? preprints of the Joint American Control Conference, San Francisco, CA, 1980, WA2-A.